

White paper: Technical-scientific Informative ITC-06 / ATCP

Elastic Moduli characterization of composites using the Impulse Excitation Technique

ATCP Physical Engineering
Sonelastic Division
www.sonelastic.com

Authors:

Lucas Barcelos Otani (Otani, L.B.)¹

Antônio Henrique Alves Pereira, PhD (Pereira, A.H.A.)¹

Revision:

José Daniel Diniz Melo, PhD (Melo, J.D.D.)²

Sandro Campos Amico, PhD (Amico, S.C.)³

(¹) ATCP Physical Engineering

(²) Federal University of Rio Grande do Norte

(³) Federal University of Rio Grande do Sul

Revision 1.4
August 18th, 2017

TABLE OF CONTENTS

1. Objective	1
2. Introduction	1
3. Elastic moduli characterization of composites using Impulse Excitation Technique	3
3.1. Technique foundations	3
3.2. Vibration modes	4
3.3. Elastic moduli of composites	6
3.3.1. Young's modulus	7
3.3.2. Shear modulus	8
3.3.3. Poisson's ratio	8
4. Correlation between material type and the elastic moduli obtained by Sonelastic®	10
5. Final Considerations	11
6. References	12
Appendix A – Elasticity Theory applied to composite materials.....	13
1. Introduction	13
2. Stiffness matrix for different material types	15
3. Micromechanical analysis	17
4. Macromechanical analysis	21
Appendix B - Poisson's ratio for different composite types employing the Impulse Excitation Technique	32
1. Isotropic material.....	32
2. Transversely isotropic material	33
3. Orthotropic material	34
Appendix C – Frequently asked questions (FAQ)	36

1. Objective

The goal of this white paper is to present the theory and methodology for the non-destructive elastic moduli characterization of composites using the Impulse Excitation Technique (ASTM E1876 [1] and correlated). This study presents a literature review and the advances achieved by ATCP Physical Engineering in what regards the application of this characterization technique applied to composites.

2. Introduction

The definition of composite materials varies according to each author, depending on the aspects and considerations that are taken into account. According to Chawla [2], for a material to be classified as a composite, it should comply with some conditions. First, it must be manufactured, meaning that it must be projected and produced by man; in addition, it must consist of an adequate combination of distinct physical and/or chemical phases; lastly, its characteristics are not achieved by any of the isolated components.

Intrinsic composite materials comprise at least two components: the matrix, which can be ceramic, metallic or polymeric; and the reinforcement, which may be in fiber or particle form. Structural composites, on the other hand, may be laminates or sandwich panels (Figure 1).

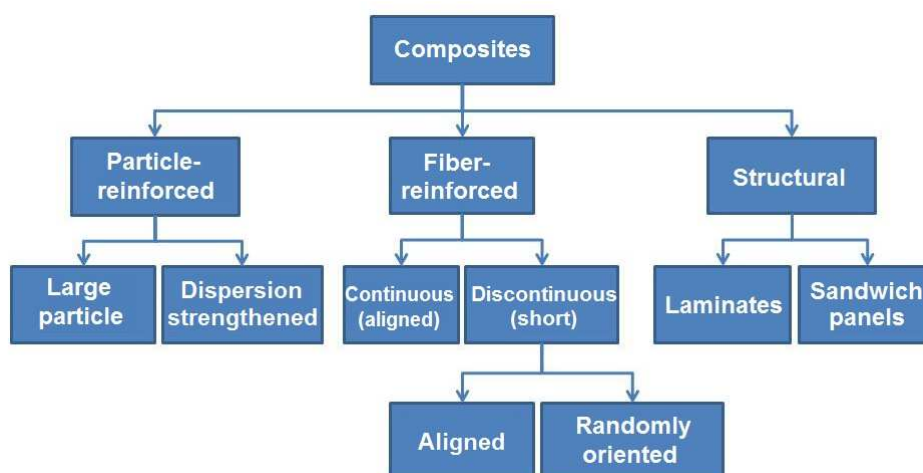


Figure 1 - Classification of composite materials [3].

The advent of composites to a place of higher technological level began in the 1960s because of a demand for materials that present high resistance allied to low density. The main areas of application included the civil construction sector, the aerospace and the power industry [2,4]. Currently, composites are used in several industries, being employed to manufacture a wide range of products from simple artifacts to high-performance cars (Figure 2). Figure 3 presents the main industries that consume polymers to manufacture composites in 2012 (data regarding the Brazilian market).



Figure 2 - Formula 1 car (2010), by Ferrari. Chassis and cockpits are currently manufactured by composite materials to ensure higher safety and lightness [5].

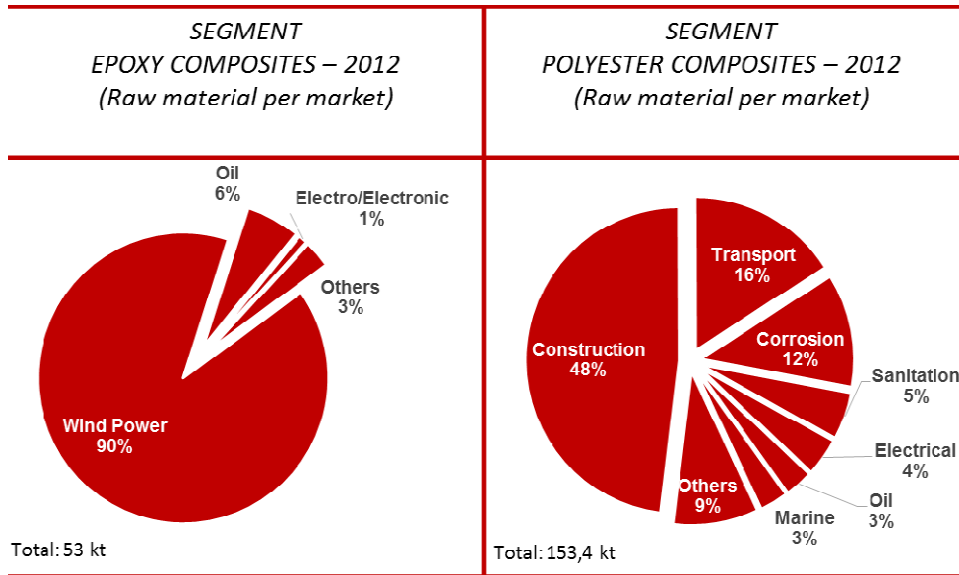


Figure 3 - Consumer market of polymers for the manufacture of composites in Brazil [6].

The elastic properties characterization of composites is crucial for the correct materials selection, numerical simulations and reliable structural calculations. One of the non-destructive techniques used to evaluate the elastic moduli and has been growing within this sector is the Impulse Excitation Technique, which is the focus of this work.

3. Elastic moduli characterization of composites using the Impulse Excitation Technique

3.1. Technique foundations

The Impulse Excitation Technique (ASTM E1876 [1]) consists in determining the elastic moduli of a material based on the natural frequency of a regular geometry sample (bar, cylinder, disc or ring). These frequencies are excited by a short mechanical impulse, followed by the acquisition of the acoustic response using a microphone. After that, a mathematical treatment is performed to the acoustic signal in order to obtain the frequency spectrum (Fast Fourier Transform). Based on this, the dynamic elastic moduli are calculated using equations provided by the ASTM standard, which considers the geometry, mass, sample dimensions and frequencies obtained through the equipment [1].

For the excitation of a desired vibration mode, it is necessary to set up specific boundary conditions. Figure 4 presents a sample holder system with the impulse device and microphone positioned to measure the Young's modulus of a rectangular bar through the flexural vibration mode.

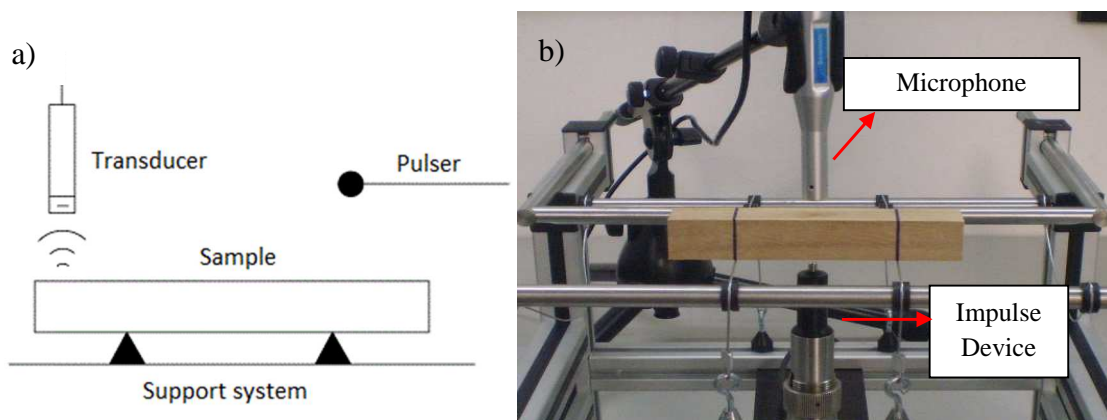


Figure 4 - a) Basic set up for the characterization of a bar through the flexural vibration mode using the Impulse Excitation Technique [7] and b) SA-BC: adjustable support for bars and cylinders.

3.2. Vibration modes

A specimen may vibrate in different ways and for each mode there is a specific fundamental frequency. Figure 5 presents the main fundamental vibration modes [8].

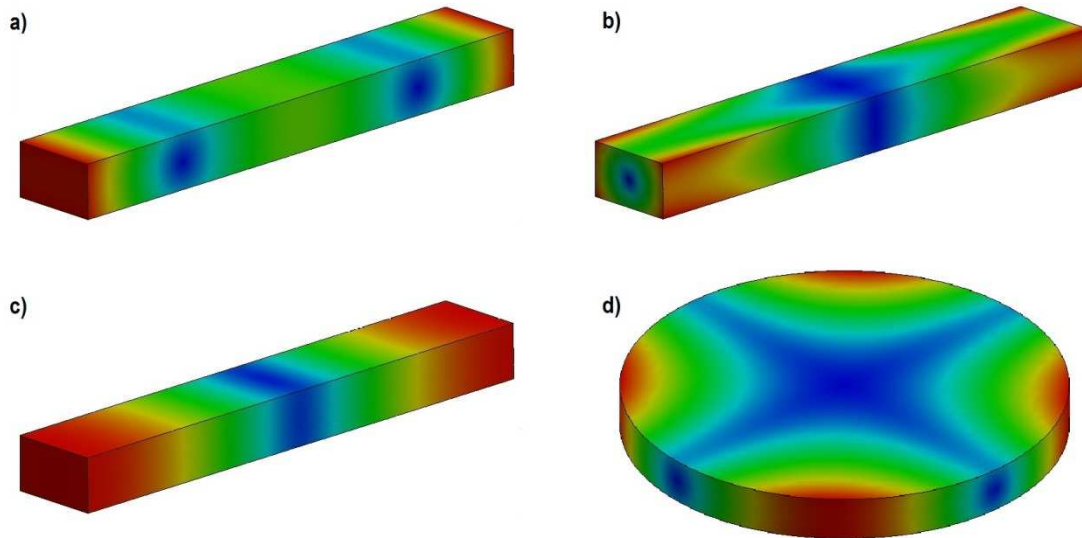


Figure 5 - Fundamental vibration modes: a) flexural, b) torsional, c) longitudinal and d) planar. Blue areas represent the regions of minimum amplitude of vibration, whilst the red areas represent the regions of maximum amplitude of vibration.

The boundary conditions determine the mode that the sample will vibrate. The natural frequencies for these modes depend on the geometry, mass, dimensions and elastic moduli.

Figure 6 a-c [1, 6] shows the optimum boundary conditions for the main vibration modes of a rectangular bar, whilst Figure 6d shows the same for a disc. Based on the resonance frequencies of the sample and by employing the equations provided by ASTM E1876 [1], it is calculated the corresponding dynamic elastic moduli.

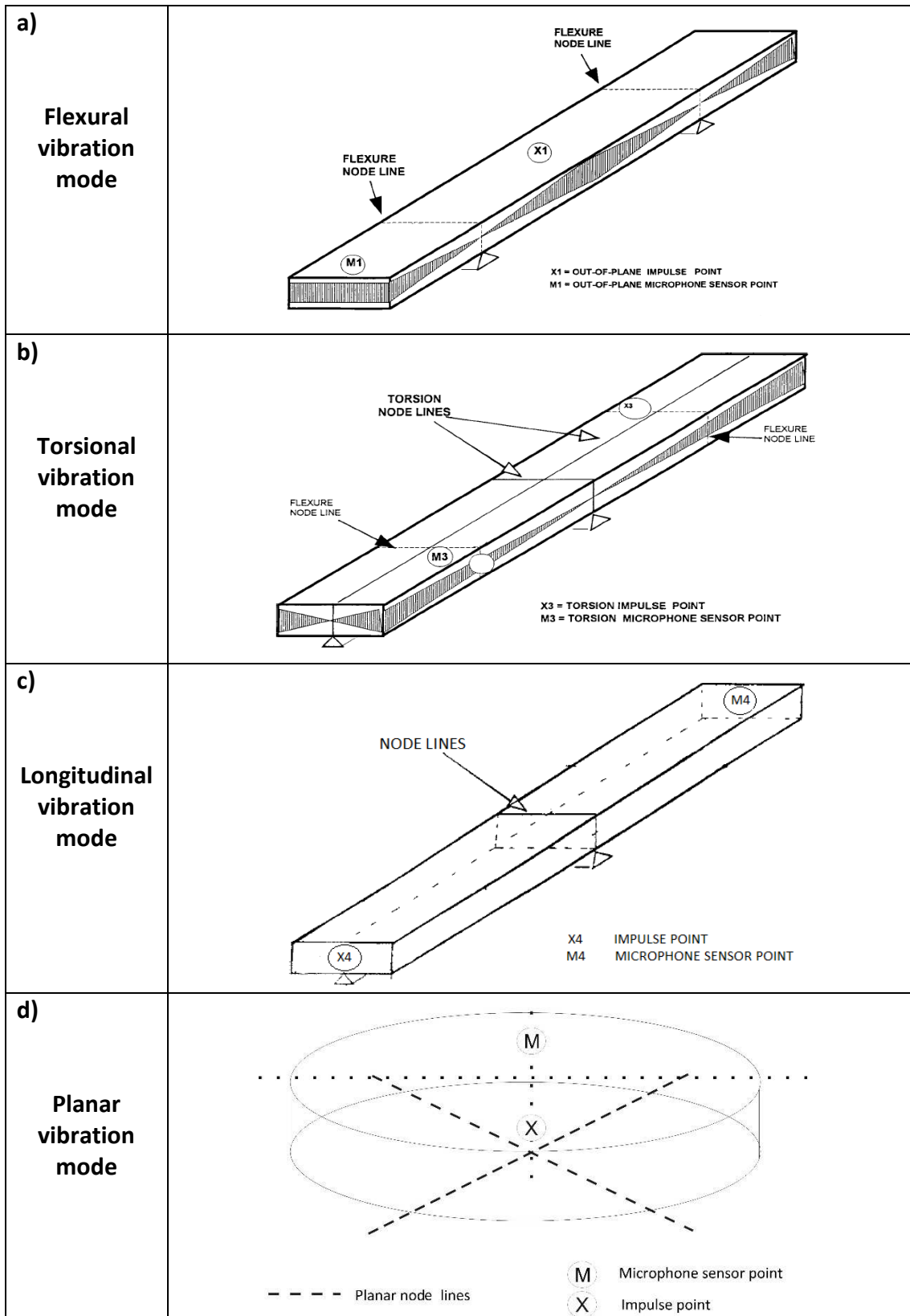


Figure 6 – Boundary conditions imposed at the sample for the excitation of the fundamental (a) flexural, (b) torsional, (c) longitudinal and (d) planar modes.

3.3. Elastic moduli of composites

The majority of composites present a certain degree of anisotropy, which means that their properties depend on the direction. Therefore, when they are characterized using the Impulse Excitation Technique, it is important to know the sample's symmetry and indicate the orientation of the excitation.

Appendix A describes the Elasticity Theory applied to composite materials based on general micro and macromechanical approaches. The appendix describes the three main material types regarding the symmetry and how the elastic constants should be dealt with in each case.

Figure 7 illustrates a non-isotropic generic structure, in which, for the characterization of the main Young's modulus (E_1, E_2, E_3) it is necessary three samples in different orientations (samples in directions 1, 2 and 3).

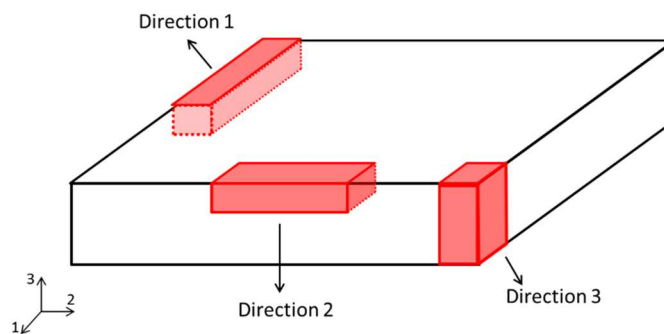


Figure 7 - Diagram of a generic structure, detailing how to obtain samples in the three main directions.

Table 1 specifies the elastic moduli that can be characterized using the Impulse Excitation Technique and their relative directions based on an orthotropic sample (Figure 7). The terms used [9] are defined as:

E_1 – Young's modulus in direction 1;

E_2 – Young's modulus in direction 2;

E_3 – Young's modulus in direction 3;

G_{eff} – Shear modulus characterized by the Sonelastic® equipment. This modulus consists of combining the G_{ij} moduli shown in parentheses [14];

G_{13} – Shear modulus associated with strains on plan 13;

G_{23} – Shear modulus associated with strains on plan 23;

G_{12} – Shear modulus associated with strains on plan 12.

Table 1 - Elastic moduli characterized by Impulse Excitation Technique in accordance to the sample orientation and the vibration mode applied.

		Vibration Mode		
		Longitudinal	Flexural	Torsional
Sample orientation	1	E_1^{long}	E_1^{flex}	$G_{eff}(G_{12}, G_{13})$
	2	E_2^{long}	E_2^{flex}	$G_{eff}(G_{12}, G_{23})$
	3	E_3^{long}	E_3^{flex}	$G_{eff}(G_{13}, G_{23})$

3.3.1. Young's modulus

- **Longitudinal vibration mode**

When the sample is loaded in longitudinal mode (check the boundary conditions in Figure 6c), the elastic modulus obtained will refer to the orientation of the sample's length. Therefore, the orientation of the sample will determine which modulus is being measured (E_1 , E_2 , E_3 or a combination of these directions), as it is presented in Table 1.

- **Flexural vibration mode**

When a material is flexed, there is both tension and compression, as pictured in Figure 8 [10]. For homogeneous and isotropic materials, the elastic modulus obtained from a bending test coincides with the elastic modulus measured in an axial test (longitudinal direction). Therefore, the value of a dynamic elastic modulus obtained using flexural vibration is the same as the one obtained using the longitudinal vibration mode [10]. Nevertheless, it is known that when flexed, the surface is the region that it is submitted to the greatest values of stress. For this reason, if a sample presents the stiffness of the surface different from the center (for example, if there is a stiffness gradient along the thickness); or if the sample presents small flaws such as pores, cracks and micro-cracks on the surface, there will be a difference between the values obtained using flexural and longitudinal modes. In the literature, there is a range of publications focused on the wood evaluation, presenting the difference between values obtained from distinct vibration modes [8, 11-13].

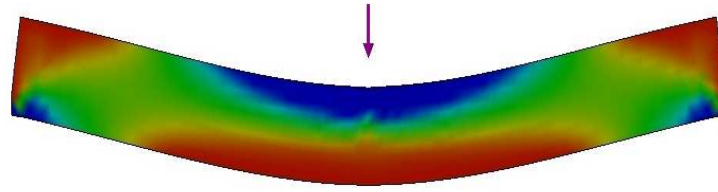


Figure 8 – Regions of tension (red) and compression (blue) stress during a bending test.

3.3.2. Shear modulus

- **Torsional vibration mode**

When a material is submitted to a torsion test, two values of shear modulus act concomitantly on materials that are transversely isotropic and orthotropic. If there is a torsion such as described in Figure 5b, the shear modulus obtained will be associated with the surfaces that are being sheared (the four lateral surfaces of the sample). Therefore, the shear modulus calculated using fundamental torsional vibration frequency correspond to an effective modulus. Thus, the results obtained by Sonelastic® will be a combination of the active shear moduli (Table 1 indicates the active shear moduli that comprise the effective value for each orientation) [14].

3.3.3. Poisson's ratio

The characterization of the Poisson's ratio using Impulse Excitation Technique occurs indirectly. It is obtained by correlating the Young's modulus and the shear modulus of a material or by the reciprocal Poisson's ratio equation. The equations come from the Elasticity Theory and are directly related to the stiffness matrices involving the symmetry present on the sample. They are shown below:

- Isotropic material:

$$\nu = \frac{E}{2G} - 1$$

- Transversely isotropic material:

$$\nu_{23} = \frac{E_2}{2G_{23}} - 1$$

- Orthotropic material:

$$\frac{\nu_{12}}{E_1} = \frac{\nu_{21}}{E_2}, \quad \frac{\nu_{13}}{E_1} = \frac{\nu_{31}}{E_3}, \quad \frac{\nu_{23}}{E_2} = \frac{\nu_{32}}{E_3}$$



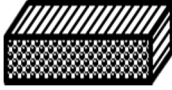

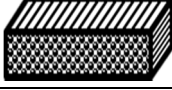

where: E is the Young's modulus; G , the shear modulus; ν , the Poisson's ratio of an isotropic material; and ν_{ij} , the negative ratio between strain in direction j and strain in direction i when a load is applied parallel to i .

Appendix B presents the source of these equations and more details explaining how to perform the characterization of Poisson's ratio using the Impulse Excitation Technique.

4. Correlation between material type and the elastic moduli obtained by Sonelastic®

As previously mentioned, composite materials may present different types of symmetry regarding their mechanical properties. Thus, it is necessary to know the kind of presented symmetry, the elastic moduli under measurement and the orientation of the sample. Table 2 shows a summary of the information presented up to this point, including details of the elastic moduli measurable by Sonelastic®.

Table 2 – Elastic moduli considering the sample’s symmetry and orientation. In addition, it is described the elastic moduli possible to be characterized through the Impulse Excitation Technique (IET).

Material type	Elastic moduli	Sample orientation		Elastic moduli characterized by the IET using Sonelastic®
Isotropic	E, G, ν	-		E, G, ν
Transversely Isotropic	$E_1, E_2 = E_3,$ $G_{12} = G_{13}, G_{23},$ $\nu_{12} = \nu_{13}, \nu_{23}$	1		$E_1, G_{12} = G_{13}$
		2 ou 3		$E_2, G_{eff} (G_{12}, G_{23})$
Orthotropic	$E_1, E_2, E_3,$ $G_{12}, G_{13}, G_{23},$ $\nu_{12}, \nu_{21},$ $\nu_{13}, \nu_{31},$ ν_{23}, ν_{32}	1		$E_1, G_{eff} (G_{12}, G_{13})$
		2		$E_2, G_{eff} (G_{12}, G_{23})$
		3		$E_3, G_{eff} (G_{13}, G_{23})$

It is possible to visualize that to characterize the measurable elastic properties using the Impulse Excitation Technique is necessary to elaborate different samples with orientations that are adequate to the material type. It is important to highlight that it is also possible to characterize samples containing fibers in intermediate angles (between 0° and 90°), and the measured properties in such directions will be in agreement with the orientation of the sample.

5. Final Considerations

Composite, materials formed by the combination of two or more materials of different nature, may be non-destructively characterized through the Impulse Excitation Technique by using Sonelastic® solutions. To do that, it is necessary to know the material type to prepare the samples according to the desired direction (main orientations, for example) and to apply the adequate boundary conditions at the characterization.

6. References

- [1] ASTM International. *Standard Test Method for Dynamic Young's Modulus, Shear Modulus, and Poisson's Ratio by Impulse Excitation of Vibration*. ASTM E1876. 2007. 15 p.
- [2] CHAWLA, K. K., *Composite Materials: Science and Engineering*. 3 ed. New York, Springer, 2012.
- [3] Translated from: composite classification. Available at: <<http://concretocomposito.blogspot.com.br/2012/06/v-behaviorurldefaultvmlo.html>>. Accessed on September 26, 2013.
- [4] DANIEL, I. M., ISHAI, O. *Engineering Mechanics of Composite Materials*. New York, Oxford University Press, 1994, 395 p.
- [5] Formula 1 car by Ferrari (2010). Available at: <http://www.f1fanatic.co.uk/2010/01/28/ferrari-2010-f1-car-pictures/ferrari_2010_3/>. Accessed on September 27, 2013.
- [6] Translated from: Compósitos: Balanço e perspectivas. Available at: <<http://www.plastico.com.br/plastico/economia/compositos-balanco-e-perspectivas/>>. Accessed on November 21, 2013.
- [7] Positioning and characterization scheme in accordance to ASTM E1876. Available at: <<http://www.atcp.com.br/pt/produtos/caracterizacao-materiais/propriedades-materiais/modulos-elasticos/metodos-caracterizacao-.html>>. Accessed on April 4, 2013.
- [8] HEYLIGER, P., UGANDER, P., LEDBETTER, H. Anisotropic Elastic Constants: Measurement by Impact Resonance. *Journal of Materials in Civil Engineering*, pp. 356-363, set/out 2001.
- [9] Adapted from WANGAARD, F.F. *The Mechanical Properties of Wood*. New York: John Wiley & Sons, Inc, 1950.
- [10] KAW, A.K. *Mechanics of composite materials*. 2 ed. Boca Raton, Taylor & Francis Group, 2006, 457 p.
- [11] ROCHA, J.S., PAULA, E.V.C.M. de, SIQUEIRA, M.L. Flexão Estática em amostras pequenas livres de defeitos. *Acta Amazonica*, Manaus, p. 147-162. 1988.
- [12] CHO, C.L., Comparison of Three Methods for Determining Young's Modulus of Wood. *Taiwan Journal for Science*, pp. 297-306, Maio/2007.
- [13] BUCUR, V., *Acoustics of Wood*. 2^a ed. Germany, Springer, 2006. p. 393.
- [14] BODIG, J., JAYNE, B. A. *Mechanics of wood and wood composites*. Malabar (EUA), Krieger Publishing Company, 1993.
- [15] GIBSON, R. F. *Principles of composite material mechanics*. USA, 1994, 425 p.
- [16] CALLISTER Jr., W.D. *Materials Science and Engineering*. 7^a ed. New York: John Wiley & Sons, Inc, 2007.
- [17] Translated from stress-strain graph. Available at: <http://www.ctb.com.pt/?page_id=1471>. Accessed on July 8, 2014.
- [18] NYE, J.F. *Physical Properties of Crystals: their representation by tensors and matrices*. Oxford: At the Clarendon Press. 1957.
- [19] TSAI, S. W. *Theory of Composites Design*. Stanford: Stanford University, 2008, 230 p.

Appendix A – Elasticity Theory applied to composite materials

1. Introduction

Based on a tensile test of an isotropic material (annealed metal, for example), at the elastic regime it is possible to correlate stress and strain as described in Equation 1 (Hooke's Law) [16]:

$$\sigma = E \cdot \varepsilon \quad (1)$$

Figure 9 shows a typical stress-strain curve of a quasi-static tensile test from which the main mechanical properties is obtained [16]. The Young's modulus, E , is the slope of the curve when the body is under the elastic regime (beginning of the curve).

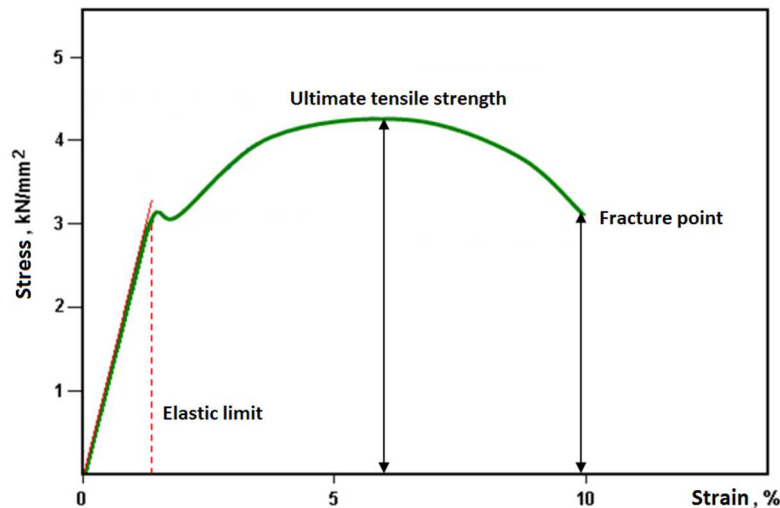


Figure 9 - Stress-strain curve of a high resistance steel [17].

It is normally acceptable to assume that composite materials present linear elastic behavior; however, in the majority of cases it is not possible to consider that these materials are isotropic [2]. For this reason, Equation 1 must incorporate indexes regarding the different directions, being the Cartesian coordinates the most used. Figure 10 shows an infinitesimal volume and stresses that may appear during loading a 1-2-3 orthogonal system.

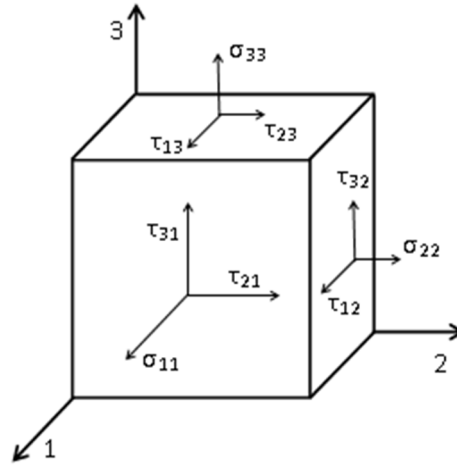


Figure 10 - Stress in an infinitesimal volume within a 1-2-3 orthogonal system.

In the presented volume, tensile stress is represented by σ and shear stress is represented by τ . Provided that there is a balance of forces within this volume, the shear stresses that are applied to the same edge of the cube should be the same (for example $\tau_{12} = \tau_{21}$). Based on these considerations, it is possible to describe the elastic behavior of an anisotropic material as:

$$\sigma_{ij} = C_{ijkl} \cdot \varepsilon_{kl}, \quad \text{in which } i, j, k, l = 1, 2, 3 \quad (2)$$

Considering the stress and the strain as square matrices of third order, it is possible to conclude that C_{ijkl} is a fourth-order tensor, known as stiffness tensor [2]. Based on the symmetry relationship described on Equation 3, it is possible to lower the number of elastic constants from 81 to 21.

$$C_{ijkl} = C_{jikl}, \quad C_{ijkl} = C_{ijlk}, \quad C_{ijkl} = C_{klij} \quad (3)$$

A reduced index notation is used to simplify the correlation between stress, strain and elastic constants, as shown in Table 3.

Table 3 – A four-index notation reduced to a two-index notation [18].

Four-index notation	11	22	33	23	31	12
Two-index notation	1	2	3	4	5	6

Based on all previous considerations, the stiffness matrix of an anisotropic material presenting linear-elastic behavior is symmetric and may be described as:

$$\begin{bmatrix} \sigma_1 \\ \sigma_2 \\ \sigma_3 \\ \tau_4 \\ \tau_5 \\ \tau_6 \end{bmatrix} = \begin{bmatrix} C_{11} & C_{12} & C_{13} & C_{14} & C_{15} & C_{16} \\ & C_{22} & C_{23} & C_{24} & C_{25} & C_{26} \\ & & C_{33} & C_{34} & C_{35} & C_{36} \\ & & & C_{44} & C_{45} & C_{46} \\ & & & & C_{55} & C_{56} \\ & & & & & C_{66} \end{bmatrix} \cdot \begin{bmatrix} \varepsilon_1 \\ \varepsilon_2 \\ \varepsilon_3 \\ \gamma_4 \\ \gamma_5 \\ \gamma_6 \end{bmatrix} \quad (4)$$

Another form to represent the stress-strain relation of a material is by using the compliance matrix, as shown below:

$$\begin{bmatrix} \varepsilon_1 \\ \varepsilon_2 \\ \varepsilon_3 \\ \gamma_4 \\ \gamma_5 \\ \gamma_6 \end{bmatrix} = \begin{bmatrix} S_{11} & S_{12} & S_{13} & S_{14} & S_{15} & S_{16} \\ & S_{22} & S_{23} & S_{24} & S_{25} & S_{26} \\ & & S_{33} & S_{34} & S_{35} & S_{36} \\ & & & S_{44} & S_{45} & S_{46} \\ & & & & S_{55} & S_{56} \\ & & & & & S_{66} \end{bmatrix} \cdot \begin{bmatrix} \sigma_1 \\ \sigma_2 \\ \sigma_3 \\ \tau_4 \\ \tau_5 \\ \tau_6 \end{bmatrix} \quad (5)$$

i.e.,

$$[S] = [C]^{-1} \quad (6)$$

It is possible to note that this model represents the elastic properties of a specific point within an object, meaning that the described constants may vary from point to point if the material is not homogeneous. Therefore, to simplify the model, despite the fact that composite materials are heterogeneous (i.e. multiphase), they are commonly considered homogeneous.

To be able to describe completely a material in what regards the elastic properties, it is necessary to find its 21 elastic constants. However, for the majority of the materials, this number is reduced because of different types of symmetry.

2. Stiffness matrix for different material types

2.1. Orthotropic material

An orthotropic material presents three mutually perpendicular planes of symmetry, in which each direction has different properties. Laminated composites formed by continuous unidirectional fibers arranged in a rectangular array and wooden bars can be classified as orthotropic materials. In this case, it is possible to verify that nine elastic constants are enough to characterize the material and the stiffness matrix will be as presented below [10]:

$$[C] = \begin{bmatrix} C_{11} & C_{12} & C_{13} & 0 & 0 & 0 \\ C_{12} & C_{22} & C_{23} & 0 & 0 & 0 \\ C_{13} & C_{23} & C_{33} & 0 & 0 & 0 \\ 0 & 0 & 0 & C_{44} & 0 & 0 \\ 0 & 0 & 0 & 0 & C_{55} & 0 \\ 0 & 0 & 0 & 0 & 0 & C_{66} \end{bmatrix} \quad (7)$$

2.2. Transversely isotropic material

Transversely isotropic materials are orthotropic materials that present isotropy in one of its planes of symmetry. Laminated composites that are formed by continuous unidirectional fibers organized in square or hexagonal array can be mentioned as examples of transversely isotropic materials. In this case, the stiffness matrix consists of five independent constants and has the following form [10]:

$$[C] = \begin{bmatrix} C_{11} & C_{12} & C_{12} & 0 & 0 & 0 \\ C_{12} & C_{22} & C_{23} & 0 & 0 & 0 \\ C_{12} & C_{23} & C_{22} & 0 & 0 & 0 \\ 0 & 0 & 0 & \frac{C_{22} - C_{23}}{2} & 0 & 0 \\ 0 & 0 & 0 & 0 & C_{66} & 0 \\ 0 & 0 & 0 & 0 & 0 & C_{66} \end{bmatrix} \quad (8)$$

2.3. Isotropic material

Isotropic materials have the characteristic to provide the same response regardless the direction in which the measurement is performed. Composites that use particulate material as reinforcement (for example glass spheres) and random short fibers within its tridimensional volume may be described by this model. In this case, the stiffness matrix will present only two independent variables and has the following form [10]:

$$[C] = \begin{bmatrix} C_{11} & C_{12} & C_{12} & 0 & 0 & 0 \\ C_{12} & C_{11} & C_{12} & 0 & 0 & 0 \\ C_{12} & C_{12} & C_{11} & 0 & 0 & 0 \\ 0 & 0 & 0 & \frac{C_{11} - C_{12}}{2} & 0 & 0 \\ 0 & 0 & 0 & 0 & \frac{C_{11} - C_{12}}{2} & 0 \\ 0 & 0 & 0 & 0 & 0 & \frac{C_{11} - C_{12}}{2} \end{bmatrix} \quad (9)$$

3. Micromechanical analysis

The micromechanical approach applied to composites consists of studying the incorporation of an amount of fibers (reinforcements) to a matrix. From the interaction and the combination between these components, it is possible to predict the elastic constants of the resultant material. The analysis is focused on how the fiber interacts with the matrix and how the stress is transferred to the reinforcement after the application of a specific stress to the composite. Tables 4 and 5 present, respectively, some properties of materials that are commonly used to manufacture composites.

Table 4 – Young’s modulus and density values for the main types of fibers used to manufacture composites [15].

Material	Type / commercial name	Young’s modulus – E (GPa)	Density (g/cm ³)
Glass fiber	E type	72	2.54
Glass fiber	S type	86	2.49
Carbon fiber (PAN)	IM-7 (Hercules)	276	1.77
Carbon fiber (PAN)	T-650/42 (Amoco)	290	1.77
Carbon fiber (tar)	P-55 (Amoco)	379	1.99
Aramid fiber	Kevlar® 29 (Dupont)	62	1.44
Aramid fiber	Kevlar® 49 (Dupont)	131	1.47
Boron fiber	D = 0.004” (Textron)	400	2.57

Table 5 – The values for Young’s modulus and density of the main types of polymeric, metallic and ceramic matrices [2].

Material	Young’s modulus – E (GPa)	Density (g/cm ³)
Epoxy	2.5 – 4.0	1.2 – 1.3
Polyester	2.0 – 4.0	1.1 – 1.4
Aluminum	70	2.7
Titanium alloy Ti-6Al-4V	110	4.5
Silicon Carbide	400 – 440	3.2
Aluminum oxide	360 – 400	3.9 – 4.0

3.1. Rule of mixtures

The rule of mixtures consists of a simplified analysis for the Young's modulus prediction of a composite formed by unidirectional fibers [2]. By applying a longitudinal load to a composite (Figure 11a), it is possible to consider that the strains in both matrix and reinforcement will be the same ($\varepsilon_c = \varepsilon_f = \varepsilon_m$). In that case, the load applied will be the sum of the loads on the matrix and on the fibers ($P_c = P_f + P_m$).

$$E_{cl} = E_f \Phi_f + E_m \Phi_m \quad (10)$$

where E_{cl} is the longitudinal Young's modulus; E_f , the fiber modulus; E_m , the matrix modulus; Φ_f , the fiber volumetric fraction present in the composite; and Φ_m , the matrix volumetric fraction in the composite ($\Phi_m = 1 - \Phi_f$).

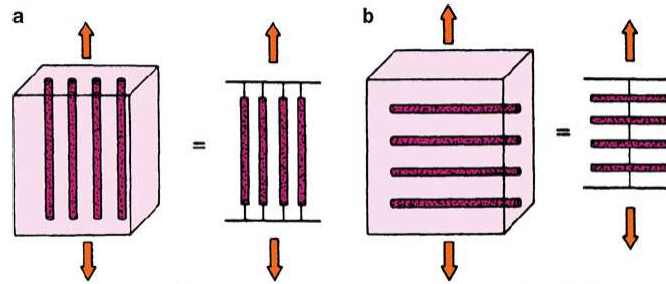


Figure 11 - Representation of a composite formed by unidirectional continuous fibers: (a) application of the load in the direction of fibers and (b) transversely to the fibers [2].

When applying a load at the transversal direction of the composite (Figure 11b), it is possible to consider that the load applied to the matrix and to the reinforcement are the same ($P_c = P_f = P_m$). In that case, the strain applied to the composite will be the sum of the strains applied to both matrix and fibers ($\varepsilon_c = \varepsilon_f + \varepsilon_m$). Thus, it is possible to come to the following equation:

$$\frac{1}{E_{ct}} = \frac{\Phi_f}{E_f} + \frac{\Phi_m}{E_m} \quad (11)$$

where E_{ct} is the transverse Young's modulus.

Equations 10 and 11 express the application of the rule of mixtures. However, this approach is not always valid because they do not take into consideration some aspects such as the reinforcement-matrix interface and the difference between the Poisson's ratio of the reinforcement and of the matrix.

- **Example of application:**

Considering a composite that is 40% formed by continuous unidirectional S-glass fibers in an epoxy resin matrix, it is possible to predict its longitudinal and transverse Young's moduli. From the values listed in Tables 4 and 5, it is possible to consider:

- $E_f = 86 \text{ GPa}$
- $E_m = 4 \text{ GPa}$

Longitudinal Young's modulus (Equation 10):

$$E_{cl} = E_f \Phi_f + E_m \Phi_m = E_f \Phi_f + E_m (1 - \Phi_f)$$

$$E_{cl} = 86 * 0.4 + 4 * (1 - 0.4) = 86 * 0.4 + 4 * 0.6$$

$$E_{cl} = 36.8 \text{ GPa}$$

Transverse Young's modulus (Equation 11):

$$\frac{1}{E_{ct}} = \frac{\Phi_f}{E_f} + \frac{\Phi_m}{E_m} = \frac{\Phi_f}{E_f} + \frac{(1 - \Phi_f)}{E_m}$$

$$\frac{1}{E_{ct}} = \frac{0.4}{86} + \frac{0.6}{4} = 0.1546$$

$$E_{ct} = 6.5 \text{ GPa}$$

Thus, the Young's modulus is approximately 36.8 GPa when the load is applied in the direction of the fibers; whilst it is approximately 6.5 GPa when the load is applied transversely to the fibers.

3.2. Halpin-Tsai equation

The Halpin-Tsai equation is a generalized form to predict the elastic properties of a composite based on the properties of matrix and fibers that are part of its composition. This equation was empirically developed and it provides satisfactory results for the composites formed by continuous and discontinuous fibers [2]. The equation has the following form:

$$\frac{p}{p_m} = \frac{1 + \xi \eta \Phi_f}{1 - \eta \Phi_f}, \quad \text{in which,} \quad \eta = \frac{p_f/p_m - 1}{p_f/p_m + \xi} \quad (12)$$

where p is the composite property (for instance, E_1 , E_2 , G_{12} or G_{23}); p_m and p_f are the matrix and fiber's properties, respectively; and ξ is a reinforcement parameter that will depend on the loading conditions, geometry and arrangement of the fibers [2].

- **Example of application:**

Considering a composite that is 40% formed by discontinuous unidirectional S-glass fibers (aspect ratio $l/d = 30$) in an epoxy resin matrix, it is possible to predict the Young's modulus of the formed material. In accordance to the values listed in Tables 4 and 5:

- $E_f = 86 \text{ GPa}$
- $E_m = 4 \text{ GPa}$

Young's modulus (Equation 12):

$$\frac{p}{p_m} = \frac{1 + \xi \eta \Phi_f}{1 - \eta \Phi_f}, \quad \text{in which} \quad \eta = \frac{p_f/p_m - 1}{p_f/p_m + \xi} \quad \text{and} \quad \xi = 2 \left(\frac{l}{d} \right)$$

the last consideration is related to composites formed by discontinuous fibers when the property being evaluated is the Young's modulus in the direction of fibers. Thus,

$$\xi = 2 \left(\frac{l}{d} \right) = 2 * 30 = 60 \quad \text{and} \quad \eta = \frac{E_f/E_m - 1}{E_f/E_m + \xi} = \frac{86/4 - 1}{86/4 + 60} = 0.2515$$

$$\frac{E}{E_m} = \frac{1 + \xi \eta \Phi_f}{1 - \eta \Phi_f} = \frac{1 + 60 * 0.2515 * 0.4}{1 - 0.2515 * 0.4} = 7.82 \text{ GPa}$$

$$E = E_m * 7.82 = 4 * 7.82 = 31.28 \text{ GPa}$$

Therefore, according to the Halpin-Tsai equation, the longitudinal Young's modulus of the composite will be approximately 31.3 GPa.

4. Macromechanical analysis

The macromechanical analysis consists on the prediction of the behavior of a laminate under shear, bending and extensional stresses. Laminates consist of stacking several laminas of some composite material in such a way that their resulting properties guarantee the desired project requirements (Figure 12). Each lamina may be identified for its position within the laminate, its material and its orientation angles in relation to the reference axis [2].

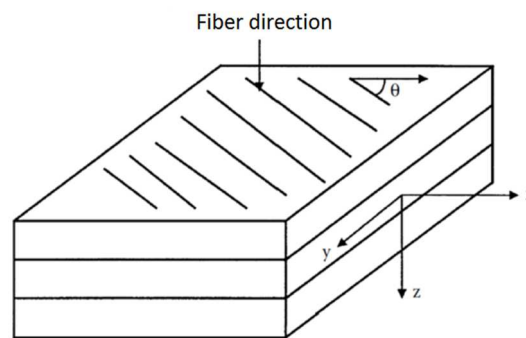


Figure 12 – Laminated composite scheme [10].

Considering that the thickness of the laminate is small in comparison to other dimensions and that there is no out-of-plane stress applied, it is possible to consider $\sigma_z = 0$, $\tau_{zx} = 0$ and $\tau_{zy} = 0$. These propositions reduce the tridimensional correlations for a bi-dimensional case [10].

To determine the stress-strain correlation of laminated composites under stress, it is normally considered that: each lamina is orthotropic and homogeneous; there is no shear in the z direction; each lamina remains under elastic regime; and there is no sliding between the layers. The origin of the coordinate system imposed will be half of the thickness and the value of z will be zero at this position (Figure 13).

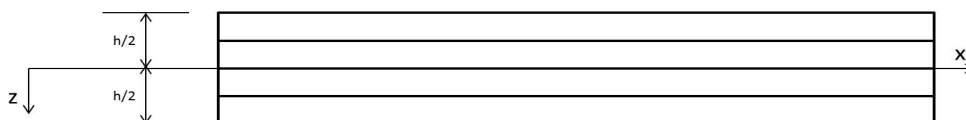


Figure 13 – Laminated composite formed by four laminas of same thickness [10].

It is considered that u_0 , v_0 and w_0 are displacement of the reference plane from the original Cartesian system in the x, y and z directions, respectively. Thus, u, v and w are the displacement from any point of x, y and z directions, respectively.

According to Figure 14, it is possible to visualize that:

$$u = u_0 - z\alpha, \text{ in which } \alpha = \frac{\partial w_0}{\partial x} \quad (13)$$

Likewise:

$$v = v_0 - z \frac{\partial w_0}{\partial y} \quad (14)$$

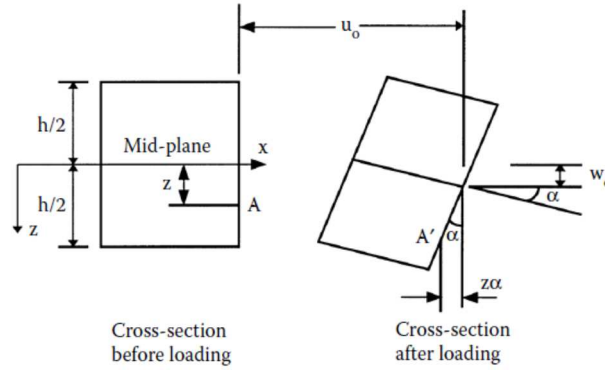


Figure 14 – Relationship between present strains within a laminated composite [10].

The definition of strains leads to:

$$\varepsilon_x = \frac{\partial u}{\partial x} = \frac{\partial u_0}{\partial x} - z \frac{\partial^2 w_0}{\partial x^2} \quad \text{and} \quad \varepsilon_y = \frac{\partial v}{\partial y} = \frac{\partial v_0}{\partial y} - z \frac{\partial^2 w_0}{\partial y^2} \quad (15)$$

$$\gamma_{xy} = \frac{\partial u}{\partial y} + \frac{\partial v}{\partial x} = \frac{\partial u_0}{\partial y} + \frac{\partial v_0}{\partial x} - 2z \frac{\partial^2 w_0}{\partial x \partial y} \quad (16)$$

Coming up to:

$$\begin{bmatrix} \varepsilon_x \\ \varepsilon_y \\ \gamma_{xy} \end{bmatrix} = \begin{bmatrix} \varepsilon_x^0 \\ \varepsilon_y^0 \\ \gamma_{xy}^0 \end{bmatrix} + z \begin{bmatrix} \kappa_x \\ \kappa_y \\ \kappa_{xy} \end{bmatrix} \quad (17)$$

where κ_x , κ_y and κ_{xy} are the midplane curvatures.

The stress matrix and the strain matrix may be correlated by the following expression:

$$\begin{bmatrix} \sigma_x \\ \sigma_y \\ \tau_{xy} \end{bmatrix} = \begin{bmatrix} \bar{Q}_{11} & \bar{Q}_{12} & \bar{Q}_{16} \\ \bar{Q}_{12} & \bar{Q}_{22} & \bar{Q}_{26} \\ \bar{Q}_{16} & \bar{Q}_{26} & \bar{Q}_{66} \end{bmatrix} \begin{bmatrix} \varepsilon_x \\ \varepsilon_y \\ \gamma_{xy} \end{bmatrix} \quad (18)$$

It must be highlighted that the reduced stiffness matrix described in Equation 18 is not formed by the same components of the stiffness matrix for the tridimensional case (Equation 4) [10].

Incorporating Equation 17 on the Equation 18 leads to:

$$\begin{bmatrix} \sigma_x \\ \sigma_y \\ \tau_{xy} \end{bmatrix} = \begin{bmatrix} \bar{Q}_{11} & \bar{Q}_{12} & \bar{Q}_{16} \\ \bar{Q}_{12} & \bar{Q}_{22} & \bar{Q}_{26} \\ \bar{Q}_{16} & \bar{Q}_{26} & \bar{Q}_{66} \end{bmatrix} \begin{bmatrix} \varepsilon_x^0 \\ \varepsilon_y^0 \\ \gamma_{xy}^0 \end{bmatrix} + z \begin{bmatrix} \bar{Q}_{11} & \bar{Q}_{12} & \bar{Q}_{16} \\ \bar{Q}_{12} & \bar{Q}_{22} & \bar{Q}_{26} \\ \bar{Q}_{16} & \bar{Q}_{26} & \bar{Q}_{66} \end{bmatrix} \begin{bmatrix} \kappa_x \\ \kappa_y \\ \kappa_{xy} \end{bmatrix} \quad (19)$$

To be able to evaluate the stress and strain state of each lamina, the stress and the bending moment may be integrated along the thickness of the laminated composite, providing the resulting forces and moments (see Figure 15).

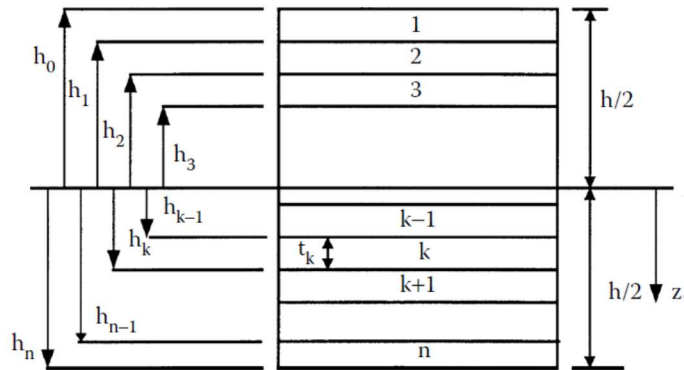


Figure 15 – Laminated composites formed by n laminae [10].

The resulting force per unit of length in the x - y plane is obtained by the integration of the global stress from all laminae along the thickness:

$$\begin{bmatrix} N_x \\ N_y \\ N_{xy} \end{bmatrix} = \int_{-h/2}^{h/2} \begin{bmatrix} \sigma_x \\ \sigma_y \\ \tau_{xy} \end{bmatrix}_k dz \quad (20)$$

In the same way, integrating the stresses in each lamina gives the resulting moments per unit of length in the x - y plane through the laminate thickness:

$$\begin{bmatrix} M_x \\ M_y \\ M_{xy} \end{bmatrix} = \int_{-h/2}^{h/2} \begin{bmatrix} \sigma_x \\ \sigma_y \\ \tau_{xy} \end{bmatrix}_k z dz \quad (21)$$

Replacing Equation 19 on Equations 20 and 21, and considering that the reduced stiffness matrix is constant for each lamina, the resulting force and moments are expressed by:

$$\begin{aligned} \begin{bmatrix} N_x \\ N_y \\ N_{xy} \end{bmatrix} &= \left\{ \sum_{k=1}^n \begin{bmatrix} \bar{Q}_{11} & \bar{Q}_{12} & \bar{Q}_{16} \\ \bar{Q}_{12} & \bar{Q}_{22} & \bar{Q}_{26} \\ \bar{Q}_{16} & \bar{Q}_{26} & \bar{Q}_{66} \end{bmatrix}_k \int_{h_{k-1}}^{h_k} dz \right\} \begin{bmatrix} \varepsilon_x^0 \\ \varepsilon_y^0 \\ \gamma_{xy}^0 \end{bmatrix} \\ &+ \left\{ \sum_{k=1}^n \begin{bmatrix} \bar{Q}_{11} & \bar{Q}_{12} & \bar{Q}_{16} \\ \bar{Q}_{12} & \bar{Q}_{22} & \bar{Q}_{26} \\ \bar{Q}_{16} & \bar{Q}_{26} & \bar{Q}_{66} \end{bmatrix}_k \int_{h_{k-1}}^{h_k} z dz \right\} \begin{bmatrix} \kappa_x \\ \kappa_y \\ \kappa_{xy} \end{bmatrix} \end{aligned} \quad (22)$$

$$\begin{aligned} \begin{bmatrix} M_x \\ M_y \\ M_{xy} \end{bmatrix} &= \left\{ \sum_{k=1}^n \begin{bmatrix} \bar{Q}_{11} & \bar{Q}_{12} & \bar{Q}_{16} \\ \bar{Q}_{12} & \bar{Q}_{22} & \bar{Q}_{26} \\ \bar{Q}_{16} & \bar{Q}_{26} & \bar{Q}_{66} \end{bmatrix}_k \int_{h_{k-1}}^{h_k} z dz \right\} \begin{bmatrix} \varepsilon_x^0 \\ \varepsilon_y^0 \\ \gamma_{xy}^0 \end{bmatrix} \\ &+ \left\{ \sum_{k=1}^n \begin{bmatrix} \bar{Q}_{11} & \bar{Q}_{12} & \bar{Q}_{16} \\ \bar{Q}_{12} & \bar{Q}_{22} & \bar{Q}_{26} \\ \bar{Q}_{16} & \bar{Q}_{26} & \bar{Q}_{66} \end{bmatrix}_k \int_{h_{k-1}}^{h_k} z^2 dz \right\} \begin{bmatrix} \kappa_x \\ \kappa_y \\ \kappa_{xy} \end{bmatrix} \end{aligned} \quad (23)$$

Knowing that:

$$\int_{h_{k-1}}^{h_k} dz = (h_k - h_{k-1}), \quad \int_{h_{k-1}}^{h_k} z dz = \frac{1}{2}(h_k^2 - h_{k-1}^2), \quad \int_{h_{k-1}}^{h_k} z^2 dz = \frac{1}{3}(h_k^3 - h_{k-1}^3)$$

The following matrix may be defined:

$$\begin{bmatrix} N_x \\ N_y \\ N_{xy} \end{bmatrix} = \begin{bmatrix} A_{11} & A_{12} & A_{16} \\ A_{12} & A_{22} & A_{26} \\ A_{16} & A_{26} & A_{66} \end{bmatrix} \begin{bmatrix} \varepsilon_x^0 \\ \varepsilon_y^0 \\ \gamma_{xy}^0 \end{bmatrix} + \begin{bmatrix} B_{11} & B_{12} & B_{16} \\ B_{12} & B_{22} & B_{26} \\ B_{16} & B_{26} & B_{66} \end{bmatrix} \begin{bmatrix} \kappa_x \\ \kappa_y \\ \kappa_{xy} \end{bmatrix} \quad (24)$$

$$\begin{bmatrix} M_x \\ M_y \\ M_{xy} \end{bmatrix} = \begin{bmatrix} B_{11} & B_{12} & B_{16} \\ B_{12} & B_{22} & B_{26} \\ B_{16} & B_{26} & B_{66} \end{bmatrix} \begin{bmatrix} \varepsilon_x^0 \\ \varepsilon_y^0 \\ \gamma_{xy}^0 \end{bmatrix} + \begin{bmatrix} D_{11} & D_{12} & D_{16} \\ D_{12} & D_{22} & D_{26} \\ D_{16} & D_{26} & D_{66} \end{bmatrix} \begin{bmatrix} \kappa_x \\ \kappa_y \\ \kappa_{xy} \end{bmatrix} \quad (25)$$

In which:

$$A_{ij} = \sum_{k=1}^n [\bar{Q}_{ij}]_k (h_k - h_{k-1}) \quad i, j = 1, 2, 6 \quad (26)$$

$$B_{ij} = \frac{1}{2} \sum_{k=1}^n [\bar{Q}_{ij}]_k (h_k^2 - h_{k-1}^2) \quad i, j = 1, 2, 6 \quad (27)$$

$$D_{ij} = \frac{1}{3} \sum_{k=1}^n [\bar{Q}_{ij}]_k (h_k^3 - h_{k-1}^3) \quad i, j = 1, 2, 6 \quad (28)$$

Based on all that has been previously exposed, it is possible to define the stress-strain relationship as:

$$\begin{bmatrix} \varepsilon^0 \\ \bar{\kappa} \end{bmatrix} = \begin{bmatrix} A^* & B^* \\ B^* & D^* \end{bmatrix} \begin{bmatrix} N \\ M \end{bmatrix} \quad \rightarrow \quad \begin{bmatrix} A^* & B^* \\ B^* & D^* \end{bmatrix}^{-1} = \begin{bmatrix} A & B \\ B & D \end{bmatrix} \quad (29)$$

Next, it is presented the equations that correlates the elastic moduli of the laminate with the thickness of the laminas and its properties. It is described the Young's moduli obtained through longitudinal and flexural vibration tests. [10].

- Young's modulus obtained through longitudinal test:

By considering the application of a load in the x direction ($N_x \neq 0, N_y = 0$ and $N_{xy} = 0$), it is possible to obtain the strain value in x through the following relation:

$$\varepsilon_x^0 = A_{11}^* \cdot N_x \quad (30)$$

Remember that $N_x = \int_{-h/2}^{h/2} \sigma_x dz = \sigma_x \cdot h$, then:

$$\varepsilon_x^0 = A_{11}^* \cdot \sigma_x \cdot h \quad \rightarrow \quad E_x^{long} = \frac{\sigma_x}{\varepsilon_x^0} = \frac{1}{A_{11}^* \cdot h} \quad (31)$$

Similarly, it is possible to come to:

$$E_y^{long} = \frac{1}{A_{22}^* \cdot h}, \quad G_{xy}^{long} = \frac{1}{A_{66}^* \cdot h}, \quad \nu_{xy}^{long} = -\frac{A_{12}^*}{A_{11}^*}, \quad \nu_{yx}^{long} = -\frac{A_{12}^*}{A_{22}^*} \quad (32)$$

- Young's modulus obtained through flexural test:

Considering the application of a bending moment in the x direction ($M_x \neq 0, M_y = 0$ and $M_{xy} = 0$), it is possible to obtain the strain value in x through the following relation:

$$\kappa_x = D_{11}^* \cdot M_x \quad \rightarrow \quad D_{11}^* = \frac{\kappa_x}{M_x} \quad (33)$$

Knowing that stress in the x direction is given by:

$$\sigma_{xx} = \frac{M \cdot z}{I} = E_x^{flex} \cdot \frac{z}{\rho} \quad \rightarrow \quad E_x^{flex} = \frac{M_x \cdot b \cdot z}{\kappa_x \cdot I \cdot z} = \frac{12 \cdot M_x \cdot b}{\kappa_x \cdot b \cdot h^3} = \frac{12}{D_{11}^* \cdot h^3} \quad (34)$$

It is also possible to come to:

$$E_y^{flex} = \frac{12}{D_{22}^* \cdot h^3}, \quad G_{xy}^{flex} = \frac{12}{D_{66}^* \cdot h^3}, \quad \nu_{xy}^{flex} = -\frac{D_{12}^*}{D_{11}^*}, \quad \nu_{yx}^{flex} = -\frac{D_{12}^*}{D_{22}^*} \quad (35)$$

- Case study – Prediction and characterization of Young’s moduli of wood laminates

Based on the described model involving macromechanic among other considerations, it is possible to predict the Young’s modulus of a laminate material from the properties of its laminas. In this study, the Sonelastic® equipment was used for the characterization of laminas and laminates produced in order to compare the theoretical value of the Young’s modulus to the experimental value obtained through the flexural and longitudinal vibration tests.

Two laminates were manufactured from wood layers divided into two groups: samples with high Young’s modulus (oriented parallel to the fibers) and samples with low Young’s modulus (oriented transversally to the fibers). For both laminates, four laminas were symmetrically bonded, so that the external laminas of *Laminate 1* consisted of laminas with greater Young’s modulus and the internal laminas with lower Young’s modulus (Figure 16a). The inverse was made to assemble the *Laminate 2* (Figure 16b).

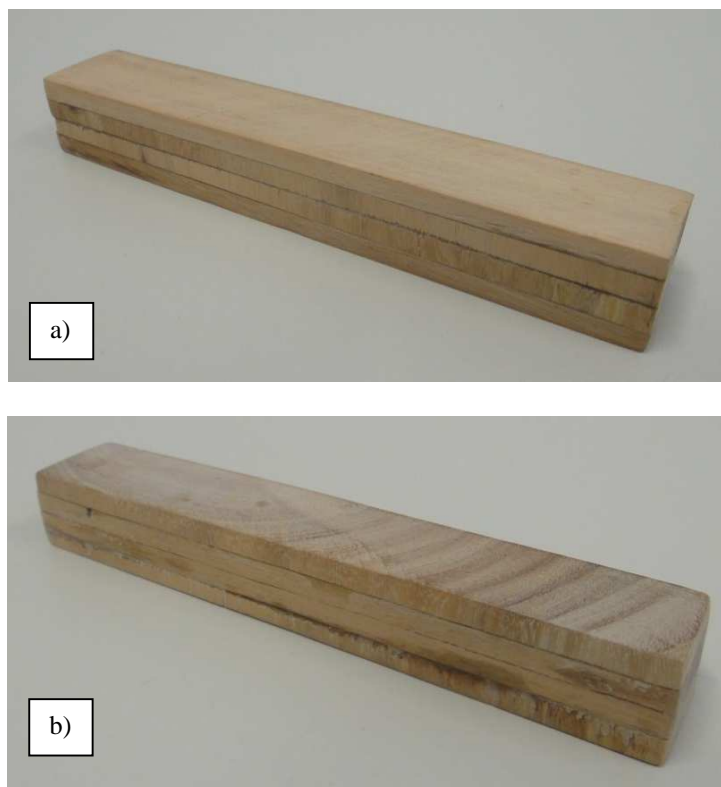


Figure 16 - (a) *Laminate 1* – external layers have greater Young’s modulus and the internal layers have lower Young’s modulus. (b) *Laminate 2* - external layers have lower Young’s modulus and internal laminas have higher Young’s modulus.

Firstly, the two groups of laminas were characterized using the Sonelastic® solutions and it was obtained an average value for them (Table 6). The mass and dimensions of the samples were measured which, together with the evaluated frequency, made possible the calculation of the Young's modulus of the material.

The SB-AP support (basic support for small samples) was employed to guarantee better conditions for the characterization of the laminas (Figure 17).



Figure 17 – Configuration of the Sonelastic solutions used to characterize the lamina in this study, highlighting the software and the basic support for small samples (SB-AP).

Table 7 presents the thickness of the laminas and their positioning.

Table 6 – Average values of Young's modulus for the two groups of laminas, obtained through [Sonelastic®](http://www.sonelastic.com).

Group	Young's modulus (GPa)	Uncertainty (GPa)	Uncertainty percentage
Wood sheets with longitudinal fibers	15.28	1.99	13.0%
Wood sheets with transversal fibers	1.49	0.09	6.0%

Table 7 – Thickness of each lamina used to make the laminates.

		Thickness (mm)
<i>Laminate 1</i>	Lamina 1	4.6
	Lamina 2	5.2
	Lamina 3	5.4
	Lamina 4	4.9
<i>Laminate 2</i>	Lamina 1	5.1
	Lamina 2	4.8
	Lamina 3	5.1
	Lamina 4	4.0

- Young's modulus prediction for *Laminate 1*:

Young's modulus obtained through longitudinal vibration mode:

According to Equation 26, neglecting the Poisson's ratio effect and considering that the reduced stiffness matrix has the same elements of the stiffness matrix (the angle of the fibers in relation to the sample's orientation is 0°), the following equations are formed:

$$A_{ij} = \sum_{k=1}^n [\bar{Q}_{ij}]_k (h_k - h_{k-1}) = \sum_{k=1}^n [Q_{ij}]_k (h_k - h_{k-1})$$

$$A_{11} = \sum_{k=1}^4 [Q_{11}]_k (h_k - h_{k-1}) = \sum_{k=1}^4 \left[\frac{E_1}{1 - \nu_{12}\nu_{21}} \right]_k (h_k - h_{k-1})$$

Considering that $\nu_{21} \rightarrow 0$, it is possible to verify that:

$$A_{11} = \sum_{k=1}^4 [E_1]_k (h_k - h_{k-1})$$

The A_{11} parameter calculation is described in Table 8.

Table 8 - A_{11} parameter calculation for *Laminate 1*.

		h_{k-1} (m)	h_k (m)	Calculation ($A_{11} \times 10^3$)	A_{11} parameter
<i>Laminate 1</i>	Lamina 1	-0.01005	-0.00545	$15.28 \times [-5.45 - (-10.05)]$	0.0703
	Lamina 2	-0.00545	-0.00025	$1.49 \times [-0.25 - (-5.45)]$	0.0077
	Lamina 3	-0.00025	0.00515	$1.49 \times [5.15 - (-0.25)]$	0.0080
	Lamina 4	0.00515	0.01005	$15.28 \times [(10.5 - 5.15)]$	0.0749
				$\Sigma =$	0.1609

Finally, considering that there is no coupling effect and using Equation 31, leads to:

$$E_x^{long} = \frac{1}{A_{11}^* \cdot h} \approx \frac{A_{11}}{h} = \frac{0.1609}{20.1 \times 10^{-3}} = 8.00 \text{ GPa}$$

Young's modulus obtained through the flexural vibration mode:

According to Equation 28, neglecting the Poisson's ratio effect of the laminas and considering again that the reduced stiffness matrix has the same elements of the stiffness matrix:

$$D_{ij} = \frac{1}{3} \sum_{k=1}^n [\bar{Q}_{ij}]_k (h_k^3 - h_{k-1}^3) = \frac{1}{3} \sum_{k=1}^n [Q_{ij}]_k (h_k^3 - h_{k-1}^3)$$

$$D_{11} = \frac{1}{3} \sum_{k=1}^4 [Q_{11}]_k (h_k^3 - h_{k-1}^3) = \frac{1}{3} \sum_{k=1}^4 \left[\frac{E_1}{1 - \nu_{12}\nu_{21}} \right]_k (h_k^3 - h_{k-1}^3)$$

Considering that $\nu_{21} \rightarrow 0$:

$$D_{11} = \frac{1}{3} \sum_{k=1}^4 [E_1]_k (h_k^3 - h_{k-1}^3)$$

D_{11} parameter calculation is described in Table 9.

Table 9 - D_{11} calculation for *Laminate 1*.

		h_{k-1} (m)	h_k (m)	Calculation ($D_{11} \times 10^9$)	D_{11} parameter
<i>Laminate 1</i>	Lamina 1	-0.01005	-0.00545	$15.28 \times [(-5.45)^3 - (-10.05)^3] / 3$	4.346×10^{-6}
	Lamina 2	-0.00545	-0.00025	$1.49 \times [(-0.25)^3 - (-5.45)^3] / 3$	8.039×10^{-8}
	Lamina 3	-0.00025	0.00515	$1.49 \times [(5.15)^3 - (-0.25)^3] / 3$	6.785×10^{-8}
	Lamina 4	0.00515	0.01005	$15.28 \times [(10.5)^3 - (5.15)^3] / 3$	4.474×10^{-6}
				$\Sigma =$	8.968×10^{-6}

Lastly, considering that there is no coupling effect and using Equation 34, leads to:

$$E_x^{flex} = \frac{12}{D_{11}^* \cdot h^3} \approx \frac{12 D_{11}}{h^3} = \frac{12 \times 8.968 \times 10^{-6}}{(20.1 \times 10^{-3})^3} = 13.25 \text{ GPa}$$

- Young's modulus prediction for *Laminate 2*:

Young's modulus obtained through longitudinal vibration mode:

According to Equation 26, neglecting the Poisson's ratio effect and considering that the reduced stiffness matrix has the same elements of the stiffness matrix (the angle of the fibers in relation to the sample's orientation is 0°):

$$A_{11} = \sum_{k=1}^4 [E_1]_k (h_k - h_{k-1})$$

The A_{11} parameter calculation is described in Table 10.

Table 10 - A_{11} parameter calculation for *Laminate 2*.

		h_{k-1} (m)	h_k (m)	Calculation ($A_{11} \times 10^3$)	A_{11} parameter
<i>Laminate 2</i>	Lamina 1	-0.0095	-0.0044	$1.49 \times [(-4.4) - (-9.5)]$	0.0076
	Lamina 2	-0.0044	0.0004	$15.28 \times [(0.4) - (-4.4)]$	0.0733
	Lamina 3	0.0004	0.0055	$15.28 \times [(5.5) - (0.4)]$	0.0779
	Lamina 4	0.0055	0.0095	$1.49 \times [(9.5) - (5.5)]$	0.0060
				$\Sigma =$	0.1648

Lastly, considering that there is no coupling effect and using Equation 31, leads to:

$$E_x^{long} = \frac{1}{A_{11}^* \cdot h} \approx \frac{A_{11}}{h} = \frac{0.1648}{19 \times 10^{-3}} = 8.67 \text{ GPa}$$

Young's modulus obtained through the flexural vibration mode:

According to Equation 28, considering that the reduced stiffness matrix has the same elements as the stiffness matrix and that $\nu_{21} \rightarrow 0$, the following equation is formed:

$$D_{11} = \frac{1}{3} \sum_{k=1}^4 [E_1]_k (h_k^3 - h_{k-1}^3)$$

D_{11} parameter calculation is described in Table 11.

Table 11 - D_{11} parameter calculation for *Laminate 2*.

		h_{k-1} (m)	h_k (m)	Calculation ($D_{11} \times 10^9$)	D_{11} parameter
<i>Laminate 2</i>	Lamina 1	-0.0095	-0.0044	$1.49 \times [(-4.4)^3 - (-9.5)^3] / 3$	3.835×10^{-7}
	Lamina 2	-0.0044	0.0004	$15.28 \times [(0.4)^3 - (-4.4)^3] / 3$	4.342×10^{-7}
	Lamina 3	0.0004	0.0055	$15.28 \times [(5.5)^3 - (0.4)^3] / 3$	8.471×10^{-7}
	Lamina 4	0.0055	0.0095	$1.49 \times [(9.5)^3 - (5.5)^3] / 3$	3.432×10^{-7}
				$\Sigma =$	2.008×10^{-6}

Finally, considering that there is no coupling effect and using Equation 34, leads to:

$$E_x^{flex} = \frac{12}{D_{11}^* \cdot h^3} \approx \frac{12 D_{11}}{h^3} = \frac{12 \times 2.008 \times 10^{-6}}{(19 \times 10^{-3})^3} = 3.51 \text{ GPa}$$

From the values obtained through the macromechanical model (described above), it was possible to compare them to the experimental values obtained using the Impulse Excitation Technique (Sonelastic®), such as presented in Table 12. The SA-BC support (adjustable support for bars and cylinders) was used in experimental characterization to provide the best conditions for the excitation of the desired vibration modes.

Table 12 - Comparison between the values obtained through the theoretical model and Sonelastic®.

		Young's modulus (GPa)		Deviation (GPa)	Percent Deviation (%)
		Macromechanical model	Sonelastic®		
<i>Laminate 1</i>	E_x^{long}	8.00	10.29	2.29	22.2%
	E_x^{flex}	13.25	14.38	1.13	7.8%
<i>Laminate 2</i>	E_x^{long}	3.51	3.60	0.09	2.5%
	E_x^{flex}	8.67	9.78	1.11	11.3%

The theoretical values described herein allow a reasonable approximation to the experimental values measured through the Impulse Excitation Technique. The deviation found is mainly due to the approximations made and the influence of the uncertainties related to the Young's modulus and dimensions that fed the model. Table 8 indicates that the initial uncertainty of the Young's modulus was approximately 13% for the laminas with longitudinal fibers and approximately 6% for the laminas with transversal fibers.

Appendix B - Poisson's ratio for different composite types employing the Impulse Excitation Technique

The characterization of the Poisson's ratio of any material using the Sonelastic® equipment must take into consideration the type of symmetry that the sample has. Despite the fact that ASTM E1876 describe the Impulse Excitation Technique only for isotropic materials [1], the technique may be extended to other material types. In that case, caution must be taken regarding the orientation of the samples.

1. Isotropic material

Only two independent variables are needed to characterize an isotropic material in what regards its elastic properties. For this reason, characterizing only one sample is enough to determine the Poisson's ratio. In this case, the compliance matrix has the following form:

$$[S] = \begin{bmatrix} S_{11} & S_{12} & S_{12} & 0 & 0 & 0 \\ S_{12} & S_{11} & S_{12} & 0 & 0 & 0 \\ S_{12} & S_{12} & S_{11} & 0 & 0 & 0 \\ 0 & 0 & 0 & 2(S_{11} - S_{12}) & 0 & 0 \\ 0 & 0 & 0 & 0 & 2(S_{11} - S_{12}) & 0 \\ 0 & 0 & 0 & 0 & 0 & 2(S_{11} - S_{12}) \end{bmatrix} \quad (36)$$

By applying the boundary conditions to the model and making some considerations [4,19], the stiffness matrix has the following form:

$$[S] = \begin{bmatrix} \frac{1}{E} & -\frac{\nu}{E} & -\frac{\nu}{E} & 0 & 0 & 0 \\ -\frac{\nu}{E} & \frac{1}{E} & -\frac{\nu}{E} & 0 & 0 & 0 \\ -\frac{\nu}{E} & -\frac{\nu}{E} & \frac{1}{E} & 0 & 0 & 0 \\ 0 & 0 & 0 & \frac{1}{G} & 0 & 0 \\ 0 & 0 & 0 & 0 & \frac{1}{G} & 0 \\ 0 & 0 & 0 & 0 & 0 & \frac{1}{G} \end{bmatrix} \quad (37)$$

By comparing the matrices, the following relation is obtained:

$$\frac{1}{G} = 2(S_{11} - S_{12}) \quad (38)$$

Knowing that $S_{11} = \frac{1}{E}$ and $S_{12} = -\frac{\nu}{E}$:

$$\frac{1}{G} = \frac{2(1+\nu)}{E} \rightarrow G = \frac{E}{2(1+\nu)} \rightarrow \nu = \frac{E}{2G} - 1 \quad (39)$$

The Poisson's ratio characterized by the Sonelastic[®] equipment is the one described in this item because it is the simplest form and it only needs one sample for its characterization. In that case, it is necessary to use the torsional vibration mode in order to obtain the shear modulus of the material.

2. Transversely isotropic material

Five independent constants are necessary to fully characterize the elastic properties of a transversely isotropic material. Next, it is presented the compliance matrix to this type of material:

$$[S] = \begin{bmatrix} S_{11} & S_{12} & S_{12} & 0 & 0 & 0 \\ S_{12} & S_{22} & S_{23} & 0 & 0 & 0 \\ S_{12} & S_{23} & S_{22} & 0 & 0 & 0 \\ 0 & 0 & 0 & 2(S_{22} - S_{23}) & 0 & 0 \\ 0 & 0 & 0 & 0 & S_{55} & 0 \\ 0 & 0 & 0 & 0 & 0 & S_{55} \end{bmatrix} \quad (40)$$

By applying the boundary conditions to the model and making some considerations [4,19], the stiffness matrix has the following form:

$$[S] = \begin{bmatrix} \frac{1}{E_1} & -\frac{\nu_{12}}{E_1} & -\frac{\nu_{12}}{E_1} & 0 & 0 & 0 \\ -\frac{\nu_{12}}{E_1} & \frac{1}{E_2} & -\frac{\nu_{23}}{E_2} & 0 & 0 & 0 \\ -\frac{\nu_{12}}{E_1} & -\frac{\nu_{23}}{E_2} & \frac{1}{E_2} & 0 & 0 & 0 \\ 0 & 0 & 0 & \frac{1}{G_{23}} & 0 & 0 \\ 0 & 0 & 0 & 0 & \frac{1}{G_{13}} & 0 \\ 0 & 0 & 0 & 0 & 0 & \frac{1}{G_{12}} \end{bmatrix} \quad (41)$$

By comparing these matrices, the following relation is obtained:

$$\frac{1}{G_{23}} = 2(S_{22} - S_{23}) \quad (42)$$

Knowing that: $S_{22} = \frac{1}{E_2}$ and $S_{23} = -\frac{\nu_{23}}{E_2}$:

$$\frac{1}{G_{23}} = 2 \left(\frac{1}{E_2} + \frac{\nu_{23}}{E_2} \right) \rightarrow G_{23} = \frac{E_2}{2(1+\nu_{23})} \rightarrow \nu_{23} = \frac{E_2}{2G_{23}} - 1 \quad (43)$$

Observing Equation 43, it is noticeable that it is not possible to obtain the Poisson's ratio (ν_{23}) only through the Impulse Excitation Technique. This can be explained because it is only possible to obtain the Young's moduli (E_1 and E_2) and the shear modulus G_{12} ($= G_{13}$) for samples presenting this symmetry.

3. Orthotropic material

Nine constants are needed to fully characterize orthotropic materials in what regards its elastic properties. Next, it is presented the compliance matrix for this type of material:

$$[S] = \begin{bmatrix} S_{11} & S_{12} & S_{13} & 0 & 0 & 0 \\ S_{12} & S_{22} & S_{23} & 0 & 0 & 0 \\ S_{13} & S_{23} & S_{33} & 0 & 0 & 0 \\ 0 & 0 & 0 & S_{44} & 0 & 0 \\ 0 & 0 & 0 & 0 & S_{55} & 0 \\ 0 & 0 & 0 & 0 & 0 & S_{66} \end{bmatrix} \quad (44)$$

By applying the boundary conditions to the model and making some considerations [4,19], the stiffness matrix has the following form:

$$[S] = \begin{bmatrix} \frac{1}{E_1} & -\frac{\nu_{21}}{E_2} & -\frac{\nu_{31}}{E_3} & 0 & 0 & 0 \\ -\frac{\nu_{12}}{E_1} & \frac{1}{E_2} & -\frac{\nu_{32}}{E_3} & 0 & 0 & 0 \\ -\frac{\nu_{13}}{E_1} & -\frac{\nu_{23}}{E_2} & \frac{1}{E_3} & 0 & 0 & 0 \\ 0 & 0 & 0 & \frac{1}{G_{23}} & 0 & 0 \\ 0 & 0 & 0 & 0 & \frac{1}{G_{13}} & 0 \\ 0 & 0 & 0 & 0 & 0 & \frac{1}{G_{12}} \end{bmatrix} \quad (45)$$

By considering the symmetry of the matrix (Equation 45), the following relation is obtained:

$$\frac{\nu_{12}}{E_1} = \frac{\nu_{21}}{E_2}, \quad \frac{\nu_{13}}{E_1} = \frac{\nu_{31}}{E_3}, \quad \frac{\nu_{23}}{E_2} = \frac{\nu_{32}}{E_3} \quad (46)$$

In that case, by characterizing three samples, one for each of the main directions, it is possible to obtain the three Young's moduli (E_1 , E_2 and E_3). Considering this, it is possible to correlate the ratio of these measurements with the material Poisson's ratio, even if it is not possible to directly obtain these properties.

Appendix C – Frequently asked questions (FAQ)

- Which geometry should the samples be prepared?

ASTM E1876 describes the equations for some specific geometries such as bars, cylinders, discs and rings. In general, for bars and cylinders, it is possible to characterize E, G and ν ; for discs and rings, it is possible to characterize the Young's modulus (E).

- How should the orientation of fibers be considered when characterizing and reporting results?

The characterization should be performed and the results reported considering the main direction of the fibers in accordance to the sample. Check if the sample is oriented in 1, 2 or 3 direction, or in a combination of directions (see chapter 3, item 3.3).

- Which Poisson's ratio value should be used to calculate the Young's modulus?

Considering that the composites are generally orthotropic materials, it is not possible to obtain results for the Poisson's ratio using this technique (Appendix B). Therefore, it is necessary to estimate a value for this property. The suggestion involves using a Poisson's ratio of 0.25 ± 0.15 to be able to cover all possible measurements. It is worthy to emphasize that, in general, the sensitivity of Young's modulus measurements in relation to the estimated Poisson's ratio is low.

- How should the sample be supported and excited?

The boundary conditions are determined according to the vibration mode required to measure the elastic moduli. If the goal is to obtain values for Young's modulus, the boundary conditions should prioritize flexural or longitudinal vibration modes. However, if the goal is to obtain values for shear modulus, boundary conditions should prioritize the torsional vibration mode (see chapter 3, item 3.2).

- How is it possible to calculate the shear modulus using effective values?

The correlation involving these properties is not trivial and it will depend on several factors. For example, a parallel combination of these properties was described for cylindrical wooden samples at [14].